Characterization of Subwavelength Grating Waveguides with 3D Finite Element Method

Yuri H. Isayama[1], Marcos S. Gonçalves[2] *IEEE Member*, Hugo E. Hernández-Figueroa[1] *IEEE Senior Member*

1 Dept. of Microwave and Optics, School of Electrical and Computer Engineering, University of Campinas, Campinas, Brazil. Email: {yurihi, hugo}@dmo.fee.unicamp.br

2 School of Technology, University of Campinas, Limeira, Brazil. Email: marcos@ft.unicamp.br

***Abstract*—A subwavelength grating waveguide was numerically analyzed by a 3D finite element method. Waveguide parameters as core height, width, duty cycle, and index contrast were varied and its effects investigated. Frequency shifts of the order of 40THz were obtained for the dispersion relation.**

I. Introduction

A subwavelength grating (SWG) waveguide confines light through index-guiding, with a core composed of alternating segments of a material of high refractive index and a material with lower refractive index. Due to the small size of the grating pitch, Bragg condition is not satisfied and diffraction is frustrated [1].

The core height of a SWG waveguide has dimensions comparable to its width and, because of that, a 2D approach of the problem might be imprecise and, thus, a 3D analysis is necessary to investigate the characteristics of these waveguides. In this work, we present a 3D finite element method (FEM) approach to analyze the effects of changes in the SWG waveguide core height, width, duty cycle, and refractive index of the core over its modal behavior.

II. Formulation

The vector wave equation for the electric field in the frequency domain is given by

$$\nabla \times \nabla \times \mathbf{E}\left(\mathbf{r}\right) = \left(\frac{\omega}{\mathrm{c}}\right)^2 \epsilon\left(\mathbf{r}\right) \mathbf{E}\left(\mathbf{r}\right), \tag{1}$$

where $\mathbf{r}$ is the position vector, $\epsilon(\mathbf{r})$ is the electric permittivity, $\mathbf{E}(\mathbf{r})$ is the electric field, and c is the speed of light in vacuum. Assuming a periodic structure, the electric field can be written as [2] $\mathbf{E(r)} = \mathbf{u(r)}\mathrm{e}^{-\mathrm{j}\mathbf{k}\cdot\mathbf{r}}$, where $\mathbf{k}$ is the wave vector, $\mathbf{u}(\mathbf{r})$ is a periodic function defined as $\mathbf{u}\left(\mathbf{r}\right) = \mathbf{u}\left(\mathbf{r}+\mathbf{a}\right)$, and and $\mathbf{a}$ is the lattice vector. Using the given definition of $\mathbf{E(r)}$ in (1), applying Galerkin's Method [3], and both the Divergence and Green's theorems, we have

$$\begin{aligned}\iiint_V \Big\{\nabla \times \mathbf{u(r)} \cdot \nabla \times \mathbf{w(r)} - \mathrm{j}\mathbf{k} \times \mathbf{u(r)} \cdot \nabla \times \mathbf{w(r)} + \\ +\mathrm{j}\mathbf{k} \times \mathbf{w(r)} \cdot \nabla \times \mathbf{u(r)} + \mathbf{k} \times \mathbf{u(r)} \cdot \mathbf{k} \times \mathbf{w(r)}\Big\}\mathrm{dV} + \\ + \oiint_S \Big\{\mathbf{w(r)} \times [\mathrm{j}\mathbf{k} \times \mathbf{u(r)} - \nabla \times \mathbf{u(r)}]\Big\} \cdot \mathbf{n}\mathrm{dS} = \\ = \left(\frac{\omega}{\mathrm{c}}\right)^2 \iiint_V \epsilon\mathbf{(r)u(r)} \cdot \mathbf{w(r)}\mathrm{dV}, \end{aligned} \tag{2}$$

where $\mathbf{w(r)}$ represents a proper trial function, V is the whole domain volume, and $\mathbf{n}$ is the unit normal vector with respect to the surface S of the computational domain.

For perfect electric conductor (PEC) and perfect magnetic conductor (PMC) boundary conditions, the surface integrals in (2) over the boundaries are zero. For periodic boundary conditions, the fields on two parallel surfaces at the boundaries of the domain must be the same and, since the normal vectors of two parallel surfaces have opposite directions, the surface integrals of (2) on two parallel surfaces must be zero.

Applying the FEM and considering the aformentioned boundary conditions, the following eigenvalue problem arises:

$$\left[\mathrm{K}\right]\left\{u\right\} = \left(\frac{\omega}{\mathrm{c}}\right)^2 \left[\mathrm{M}\right]\left\{u\right\}. \tag{3}$$

The elementary matrices, related to the global matrices, are given by:

$$\begin{aligned}\left[\mathrm{K^e}\right]_{\mathrm{m,n}} = \iiint_{V_e} \Big[\nabla \times \mathbf{W}^{\mathrm{e}}_{\mathrm{m}} \cdot \nabla \times \mathbf{W}^{\mathrm{e}}_{\mathrm{n}} - \mathrm{j}\mathbf{k} \times \mathbf{W}^{\mathrm{e}}_{\mathrm{m}} \cdot \nabla \times \mathbf{W}^{\mathrm{e}}_{\mathrm{n}} + \\ +\mathrm{j}\mathbf{k} \times \mathbf{W}^{\mathrm{e}}_{\mathrm{m}} + \mathbf{k} \times \mathbf{W}^{\mathrm{e}}_{\mathrm{m}} \cdot \mathbf{k} \times \mathbf{W}^{\mathrm{e}}_{\mathrm{n}}\Big]\mathrm{dV}, \end{aligned}$$

$$\left[\mathrm{M}^{\mathrm{e}}_{\mathrm{m,n}}\right] = \iiint_{V_e} \mathbf{W}^{\mathrm{e}}_{\mathrm{m}} \cdot \mathbf{W}^{\mathrm{e}}_{\mathrm{n}}\mathrm{dV}.$$

where $\mathbf{W}^{\mathrm{e}}_{\xi}$ is the Whitney basis function. The basis function associated to the edge ξ that connects the nodes *l* and *j* is given by $\mathbf{W}^{\mathrm{e}}_{\xi} = \mathrm{L}_l\nabla\mathrm{L}_j - \mathrm{L}_j\nabla\mathrm{L}_l$, where $\mathrm{L}_{i,j}$ are nodal basis functions associated to the nodes *l* and *j*, respectively, and V_e is the volume of an element of the discretized domain.

978-1-4673-1604-0/12/$31.00 ©2012 IEEE

III. Simulation Results

The computational domain simulated had dimensions $x \times y \times z = 2\mu\text{m} \times 2\mu\text{m} \times 0.3\mu\text{m}$, and periodic conditions were applied at the planes z = 0 and z = 0.3 μm. A segmentation pitch of Λ = 0.3 μm, substrate height of 0.4 μm, and an upper cladding (air) height of 1.6 μm were employed. The refractive index of the subtrate and the upper cladding are, respectively, n_{SiO_2} = 1.44, and n_{air} = 1.0. The waveguide core is made of either Si (n_{Si} = 3.476) or Si_3N_4 ($n_{Si_3N_4}$ = 1.99).

Figs. 1 and 2 show the dispersion relation of quasi-TE and quasi-TM modes, respectively, for a core width *w* = 300 nm, refractive index $n_{Si} = 3.476$, and different values of core height (*h*) and segment length (*l*). The duty cycle of the waveguide corresponds to the ratio l/Λ. As expected, it is observed that increasing the waveguide height or width the dispersion curves of the waveguide suffer a shift to lower frequencies and the modes become more confined to the core. Increasing the duty cycle also has the effect of shifting the dispersion curves to lower frequencies and it decreases the cutoff frequency of both quasi-TE and quasi-TM modes. Increasing *w* from 300 nm to 500 nm in a *h* = 300 nm and 50% duty cycle waveguide produces a shift of 42 THz for the quasi-TE mode and 15.7 THz for the quasi-TM mode. For a *w* =300 nm and *l* = 150 nm waveguide, increasing *h* from 300 nm to 600 nm produces a shift of 14THz for TE polarization and 46 THz for TM polarization.

Fig. 3 presents the dispersion relation for the quasi-TM mode (fundamental) for different core materials (Si and Si_3N_4), *w* = 300 nm and l = 150 nm. Reducing the refractive index of the core has the effect of moving the dispersion curves to higher frequencies. The variations of the refractive index of the waveguide core, as well as the variations of waveguide width could be analyzed by a 2D approach. However, Figs. 1 and 2 show that changes in the SWG waveguide height can result in big variations in its dispersion relation and, because the effects of waveguide height are not considered in a 2D model, in order to properly investigate the waveguide presented here, a 3D formulation is fundamental.

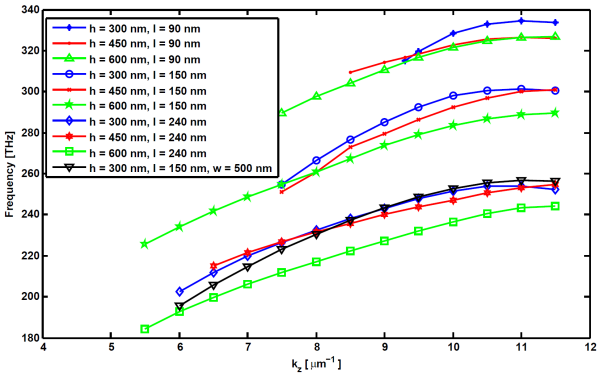

Fig. 1. Dispersion relation for the quasi-TE mode for *w* = 300 nm.

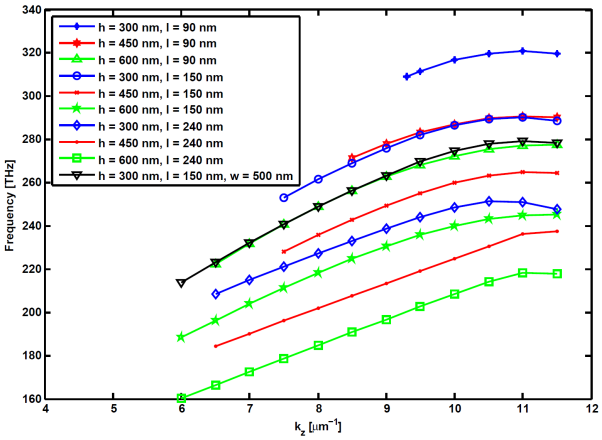

Fig. 2. Dispersion relation for the quasi-TM mode for *w* = 300 nm.

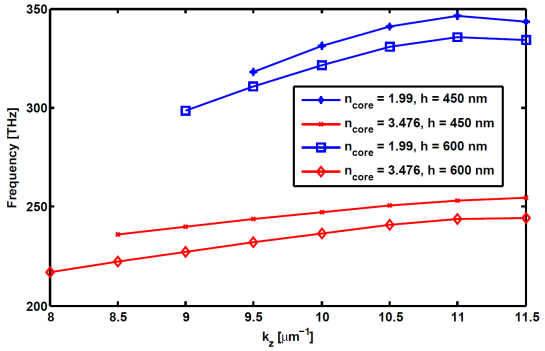

Fig. 3. Dispersion relation for the quasi-TM mode for *w* = 300 nm and *l* = 150 nm.

IV. Conclusion

In this paper, the modal characteristics of a SWG waveguide were analyzed with a 3D finite element method. Frequency shifts of the order of 40 THz were obtained, by manipulating the waveguide height, for TM polarization, and waveguide width, for TE polarization. In conclusion, it is possible to engineer the effective index not only by varying the duty cycle of the waveguide and its refractive index, but also by altering parameters as its height and width. Additionally, the possibility to produce large frequency shifts in the dispersion relation makes the SWG waveguide suitable for waveguide coupling, and, therefore, it represents an important building block for integrated optics.

Acknowledgment

This work was supported by INCT-Fotonicom, CAPES, FAPESP, and FAEPEX.

References

[1] I. Molina-Fernandez *et al.*, "New concepts in silicon component design using subwavelength structures," in *Proc. SPIE*, 2012, vol. 8266, p. 82660E.

[2] J. D. Joannopoulus, R. D. Meade, and J. N. Winn, *Photonics crystals: molding the flow of light*, Princeton University Press, 1995.

[3] J. M. Jin, *The finite element method in electromagnetics*, 2nd edition, Wiley, New York, 2002.